ISBN: 978-3-95450-212-7 ISSN: 2673-5482 doi:10.18429/JACoW-CYCLOTRONS2022-MOAI02

UPGRADE AND CURRENT STATUS OF HIGH-FREQUENCY SYSTEMS FOR RIKEN RING CYCLOTRON

K. Yamada*, RIKEN Nishina Center, Wako, Japan

Abstract

The high-frequency systems for the RIKEN Ring Cyclotron (RRC) were upgraded to increase the acceleration voltage at 18.25-MHz operation by remodeling its cavity resonators and rf controllers. After the upgrade, the maximum gap voltage at 18.25 MHz improved from about 80 kV to more than 150 kV. The beam intensity of ^{238}U for the RI Beam Factory was increased up to 117 pnA in 2020 by overcoming the beam intensity limitation of the RRC due to the space charge effect. This article presents the details of the upgrade as well as the current status of the high-frequency systems for the RRC.

INTRODUCTION

RI Beam Factory

The Radioactive Isotope Beam Factory (RIBF) [1, 2] at the RIKEN Nishina Center started operation in 2006 in order to pursue heavy-ion beam science through basic and applied research, such as determining the origin of the elements, establishing new nuclear models, synthesizing new elements and isotopes, researching nuclear transmutation, and supporting industrial applications including biological breeding and producing useful RIs. The RIBF has four separate-sector cyclotrons: the RIKEN ring cyclotron (RRC [3], K = 540 MeV), the fixed-frequency ring cyclotron (fRC [4–6], K = 700 MeV), the intermediate-stage ring cyclotron (IRC [7], K = 980 MeV), and the world's first superconducting ring cyclotron (SRC [8], K = 2600 MeV). The RIBF can provide the world's most intense RI beams for all masses by accelerating heavy-ion beams up to 70% of light speed in cw mode, using a cascade of the four ring cyclotrons combined with different types of injectors: a variable-frequency heavy-ion linac (RILAC [9, 10]), a fixed-frequency heavy-ion linac (RILAC2 [11, 12]), and a K70-MeV AVF cyclotron (AVF [13]).

Uranium is one of the most important beams in the RIBF because it can produce many rare isotopes via the in-flight fission of uranium ions by a superconducting in-flight fragment separator, BigRIPS [14]. As shown in Fig. 1, the uranium ions are produced with a powerful 28-GHz superconducting ECR ion source [15, 16] at the charge state of 35+ and accelerated through the RILAC2 and RRC up to 11 MeV/u. After changing their charge state to 64+ by a helium gas stripper [17], they are further accelerated in the fRC and converted to 86+ by a graphite sheet stripper [18]. Finally, they are boosted up to 345 MeV/u by the IRC and SRC, and directed to the BigRIPS.

* nari-yamada@riken.jp

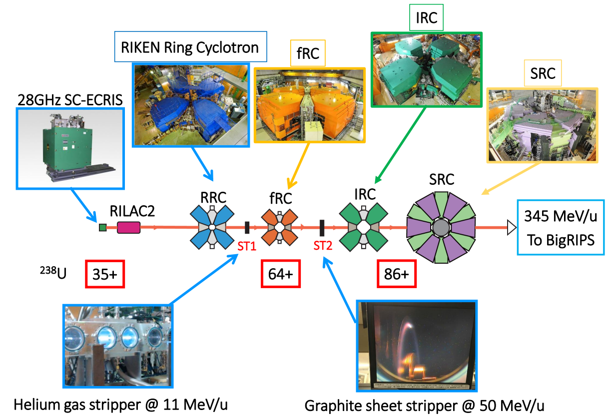

Figure 1: Schematic of uranium acceleration at the RIBF.

This article describes in detail the modification of the high-frequency systems for the RRC.

Overview of RRC

The RRC is a four-sector normal-conducting isochronous ring cyclotron that has been in operation for over 35 years. The RRC can accelerate light ions up to 135 MeV/u and is also frequently used to provide the intermediate-energy beams. Figure 2 indicates the equipment layout of the RRC. The RRC has an injection radius of 89.3 cm and an extraction radius of 356 cm, giving a large velocity gain of 4. Each radial sector has a sector angle of 50 degrees and is equipped with 26 trim coils. Beams are injected and extracted by one electrostatic deflector and two magnetic channels and bending magnets, respectively. The specifications of the RRC are summarized in Table. 1.

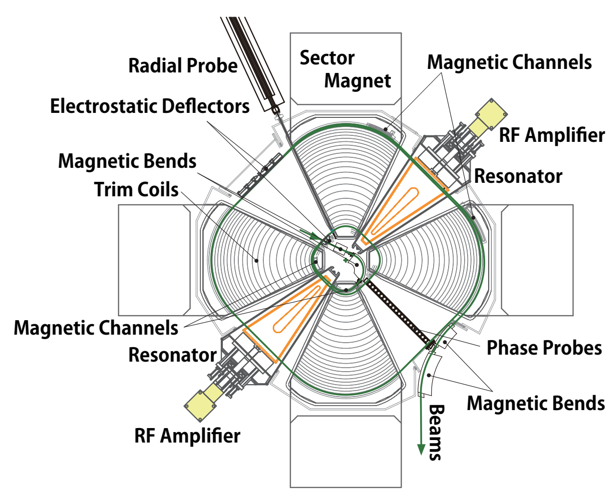

Figure 2: Equipment layout of the RRC.

ISBN: 978-3-95450-212-7 ISSN: 2673-5482 doi:10.18429/JACoW-CYCLOTRONS2022-MOAI02

Table 1: Specifications of the RRC

Parameter	Value
K-value	540 MeV
Sectors	4
Sector angle	50°
Pole gap	80 mm
Maximum field	1.6 T
Trim coils	26
Velocity gain	4.0
Mean injection radius	89 cm
Mean extraction radius	356 cm
Acceleration cavities	2
Frequency range	18–42 MHz
Harmonics	5, 9, etc.

The RRC has two variable-frequency acceleration cavities and does not use a flat-top system. The acceleration cavities of the RRC [19] are based on a half-wavelength resonator, which has two gaps between the dee electrode and the outer wall. The dee angle is 23.5 degrees, the acceleration gap length is 100 mm, and the outer dimensions of the cavity are 2.1 m(H)×3.5 m(W)×1.6 m(D). As shown in Fig. 3, the variable frequency devices of the RRC use a unique mechanism called a movable-box-type. The movable box is not in contact with the stem, only with the outer wall. The frequency can be varied using not only a change in the inductance but also the capacitance when the movable-box approaches the dee electrode. This mechanism makes it possible to vary the frequency from about 20 to 45 MHz with a size less than one-third that of a movable-short-type cavity. However, the dee voltage is frequency dependent due to the large shunt-impedance variation. The rf amplifier of the RRC is a three-stage configuration using tetrodes and has a maximum rf output of around 150 kW. The rf system has a voltage stability of less than 0.1% and a phase stability of less than 0.1 degree. We are currently using low-level circuits with analog feedback.

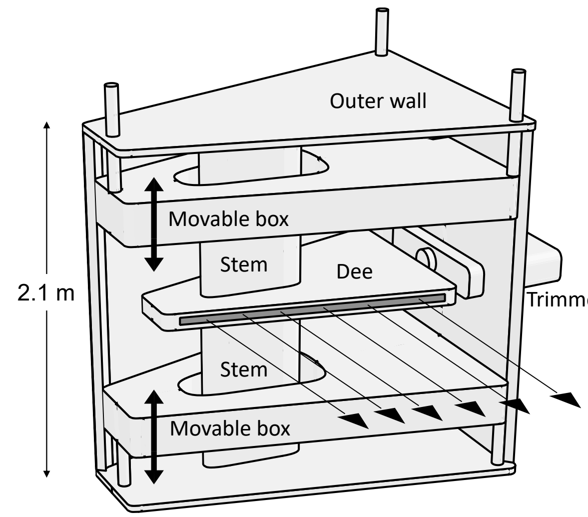

Figure 3: Schematic drawing of the movable-box-type cavity resonator for the RRC. An rf power coupler is concentric with a fine-tuner (trimmer).

UPGRADE OF HIGH-FREQUENCY SYSTEM FOR RRC

Objective of the Upgrade

As a result of many improvements [20] since the beginning of the operation of the RIBF in 2007, the beam intensity was steadily increased to nearly 1 pμA, the target value of the RIBF project, for various ion beams. However, the intensity of the uranium beam had reached a peak at about 70 pnA at the exit of the SRC in 2017, in contrast to other ion beams. The transmission efficiency of the RIBF was also increased over the years, but the beam loss at the RRC extraction on the electrostatic deflection channel (EDC) was close to reaching its limit of about 300 W. As the beam intensity supplied from upstream increased, the beam quality deteriorated due to space-charge effects in the RRC [21], resulting in increased beam loss at the RRC extraction. This was a major cause limiting the uranium beam intensity of the RIBF.

The underlying cause of this increased beam loss was the inability to obtain enough turn separation due to the insufficient acceleration voltage of the RRC. During the acceleration of very heavy ions including uranium, the rf system of RRC have to operate at 18.25 MHz. However, a gap voltage of only 85 kV could be generated at this frequency because the operation frequency of 18.25 MHz was actually out of the design specifications. For example, applying the RRC parameters to the equation reported by Baartman [22], the limit current for the uranium beam acceleration of the RRC with an rf voltage of 85 kV was derived to be 2.3 pμA. This value was close to the beam current in the RRC at that time.

The upper panel of Fig. 4 shows the calculation model with the original cavity operated at about 18.25 MHz. The gap length between the dee electrode and the movable box had to be set very small, about 20 mm beyond the design range. As a result, the maximum voltage had been limited to 85 kV, because of the frequent rf discharge caused by this small gap. The actual parallel shunt impedance was also very low, less than 40 kΩ, and the large rf input power caused a severe shock during discharge. Therefore, we decided to modify the cavity resonators to increase the acceleration voltage of the RRC.

Design and Modification of RF Components

To increase the acceleration voltage of the RRC, the gap between the dee electrode and the movable box had to be widened. As shown in the lower panel of Fig. 4, a new slanted stem structure was adopted to shift the resonance frequency range to the lower side by increasing the inductance of the resonator. The increased inductance reduced the capacitance for the same frequency, so the gap length could be almost doubled at 18.25 MHz as shown in Fig. 4. At the same time, the shunt impedance was more than doubled and thus the required rf power was significantly reduced. This modification was expected to increase the voltage at 18.25 MHz by a factor of 1.5 or more.

ISBN: 978-3-95450-212-7 ISSN: 2673-5482 doi:10.18429/JACoW-CYCLOTRONS2022-MOAI02

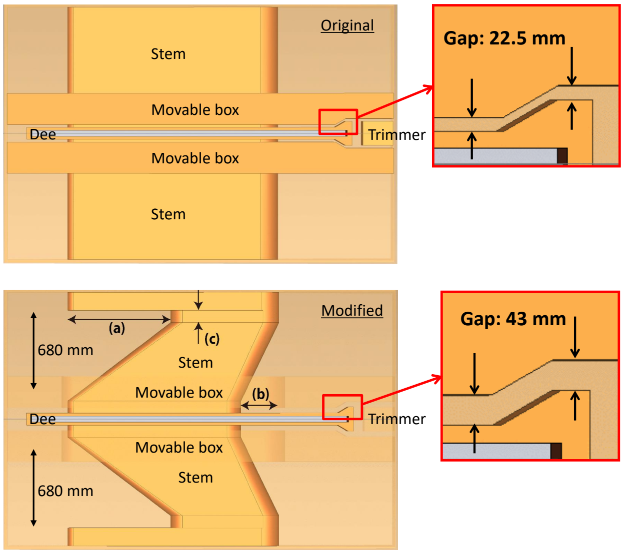

Figure 4: Calculation models of the original cavity (upper panel) and the modified cavity (lower panel).

For this modification, we decided to replace only the internal conductors, the stem and dee, and to not change other components such as the outer wall and movable box. 3D electromagnetic calculations were performed using the CST Studio Suite [23] to find the optimal geometry of the inner conductor. As shown in the lower panel of Fig. 4, the three dimensions (a), (b), and (c) were used as parameters to determine well-balanced dimensions to ensure the required frequency range was obtained while widening the gap as much as possible and increasing the shunt impedance. The calculated design parameters are summarized in Table 2 as well as the original cavity values. Since frequencies above 39 MHz are not used today, the maximum resonant frequency was designed to be less than 39 MHz. The mounting parts were made to have identical dimensions for compatibility. The distribution of heat generation obtained from the electromagnetic calculation was also used for the cooling design.

The radial voltage distribution at the acceleration gap was also taken into account with regard to maintaining the bunch compression effect by the high-frequency magnetic field [24]. Since there is no flat-top cavity in the RRC and the phase acceptance is small, acceleration with compression of the bunch is advantageous for beam extraction. From this point of view, the voltage distribution should be such that the voltage increases toward the outer circumference without any mid-range sagging, and such a distribution was obtained in the original cavity. Noted that the voltage distribution of the RRC is gentle at the low-frequency side, which affects the high-frequency side. In the calculation, dimension (b) works to compensate for the mid-range sag. The mid-range sag was not completely eliminated, but it was kept to a level that did not affect the beam acceleration.

Figure 5 shows pictures during the modification work of the RRC cavity. As shown in panel (a), the new dee electrode and stem were fabricated as four sets of half-units using

Table 2: Calculation results for the original cavity and the modified cavity. The definition of shunt impedance is $R = V_{\text{gap}}^2/2P$ here

	Original Cavity	Modified Cavity
Frequency range	20–45 MHz	16–38.8 MHz
Stroke of MBOX	680 mm each	680 mm each
Shunt impedance	61–594 kΩ	78–451 kΩ
Shunt impedance (around 18.25 MHz)	~48 kΩ	~99 kΩ
Quality factor Q_0 (around 18.25 MHz)	8865	11160
Gap length (b/w dee and MBOX)	22.5 mm	43 mm
Maximum voltage (around 18.25 MHz)	~85 kV	>120 kV

oxygen-free copper. The modification work was performed from February to March 2018, and the interior of the cavity after completion of the modification is shown in panel (d) of Fig. 5.

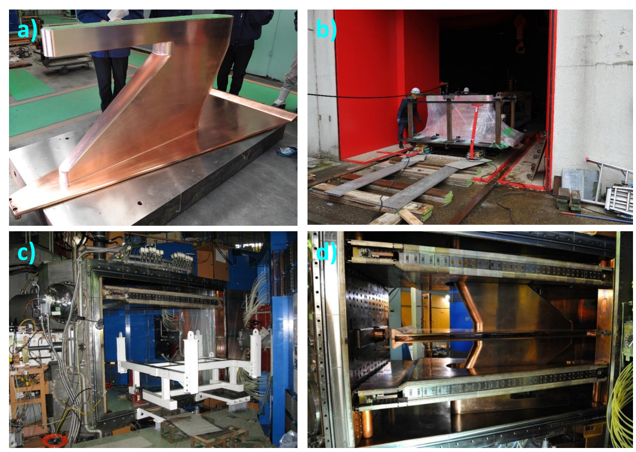

Figure 5: Photographs of the modification work, showing a new half-unit of the stem and dee electrode (a), delivery of fabrication parts (b), replacement of cavity contents (c), and completed assembly (d).

The aging rf control system and tetrode grid power supplies for the RRC were also updated before and after the cavity upgrade. The rf controller, which was implemented with hardware relay logic, was replaced by a programmable logic controller (PLC) based system. All the driving motors and motor drivers for the cavity resonators were also replaced, with only the analog low-level circuits retained. All the components are now controlled directly from the PLC, and remote operation has been moved to an Ethernet base. This renewal resulted in a faster recovery time in a trip event, less damage to the amplifiers, and improved resolution of rf voltage and phase set points. The aging grid power supplies, in use for more than 30 years, were renewed because they were beyond repair and had been unstable in re-

ISBN: 978-3-95450-212-7 ISSN: 2673-5482 doi:10.18429/JACoW-CYCLOTRONS2022-MOAI02

cent years. Since they are placed in a radiation environment, they were manufactured using a standard logic IC without using a micro-controller.

UPGRADE RESULTS AND CURRENT STATUS

After the modification, the frequency response was measured with a network analyzer in April 2018. For each movable-box position, the resonant frequency corresponding to each trimmer position is plotted in Fig. 6. Each point represents the result of a measurement and the curves indicate the calculation results for four movable-box positions. As shown in Fig. 6, the frequency response is almost exactly as expected from the calculations. No detrimental resonance peaks were observed up to 200 MHz for each operating frequency. The quality factor was also measured with a network analyzer for each frequency. The internal quality factor of each frequency is almost 80% of the calculation. This is due

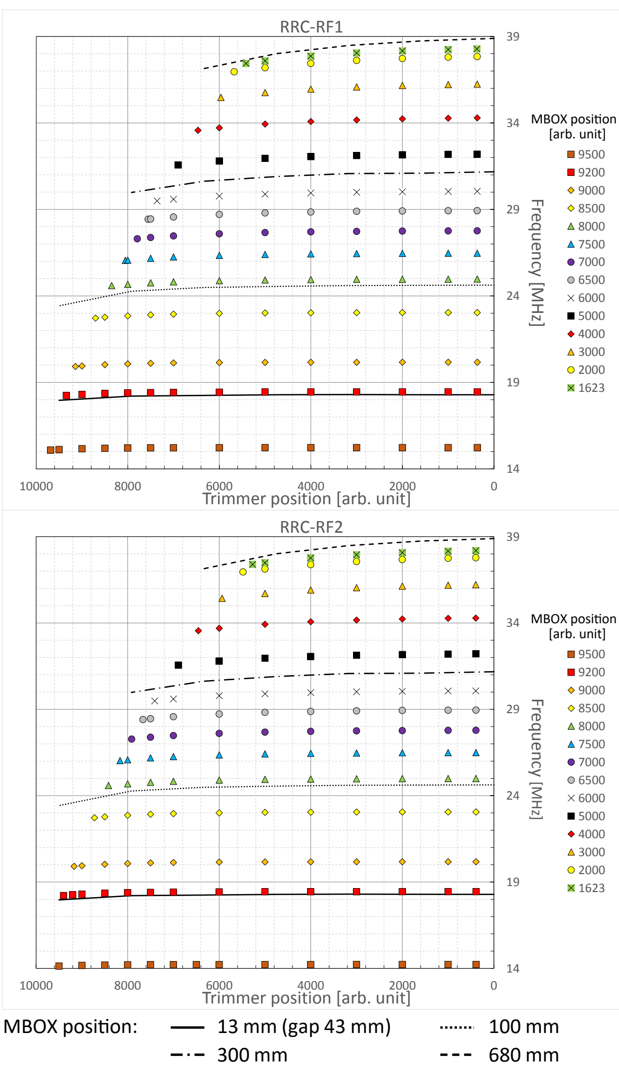

Figure 6: Resonant frequencies measured with a network analyzer for two cavities. The markers are changed according to the movable-box position.

to the many contact points of the sliding parts, however it is consistent with the value assumed in advance based on past experience.

Immediately after the low power test, we started applying high power at 32.6 MHz for conditioning. In a few hours, the voltage was up to the specified voltage of 220 kV for 32.6-MHz operation, and a week later in May 2018, the beam supply to the experiment was resumed. In the 18.25-MHz operation, the voltage was increased step by step. The maximum acceleration voltage of 160 kV was achieved at 18.25 MHz in 2020 by increasing the anode voltage of the final stage tetrode from 10 kV to 12 kV. The shunt impedance at 18.25 MHz was also more than double the previous value based on the relationship between voltage and power. Thus, it is now possible to operate the cavity at a voltage about twice as high as before at 18.25 MHz.

Figure 7 shows the radial beam pattern of the uranium accelerated in 2017 and 2020. The left side is injection and the right side is extraction. The operating voltage in 2017 was 85 kV and in 2020 it was 140 kV. As can be seen in Fig. 7, the effect of the voltage enhancement is remarkable, and the turn separation of the RRC has been significantly improved even with uranium acceleration. This increased turn separation has reduced the beam loss on the RRC EDC by a factor of three. Thus, there is now a margin for beam intensity that can be accelerated by the RRC.

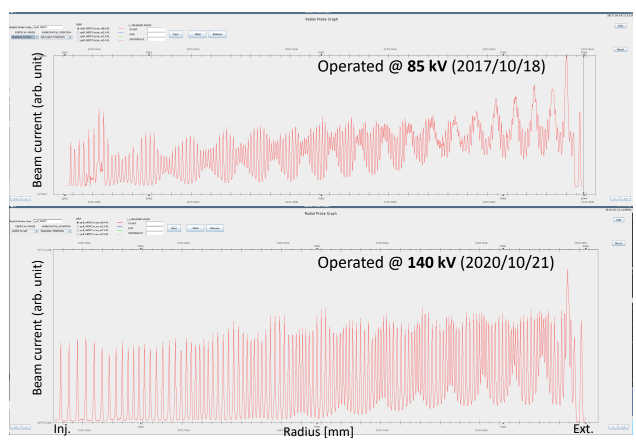

Figure 7: Radial beam pattern in the RRC for the uranium beam acceleration before (upper panel) and after modification (lower panel).

In addition, the cavity modifications significantly reduced rf discharges and resulting trips as expected. The upper panel of Fig. 8 shows the number of rf discharges-per-day and rf trips-per-day during uranium acceleration in 2017, before the cavity modification. We suffered from rf discharges about 20 to 60 times per day at around 85 kV. On the other hand, after the modification, the number of discharges has been greatly reduced to only a few times per day in spite of the higher voltage, and tripping almost never occurs, as shown in the lower panel of Fig. 8. This dramatic reduction in rf discharges also contributes to improving the beam availability of the RIBF and now exceeds 90%.

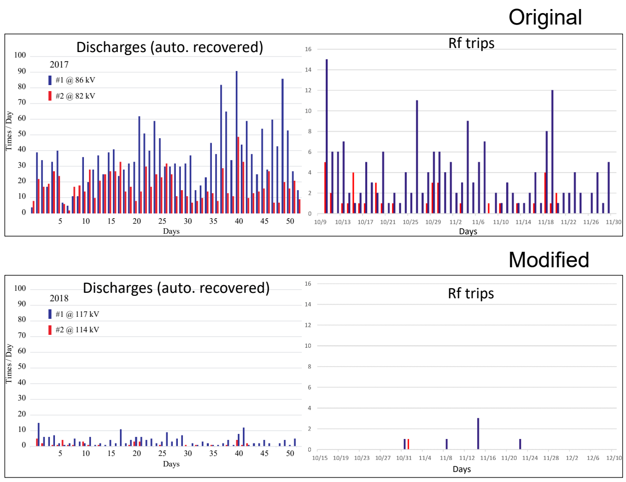

Figure 8: Comparison of rf discharges and trips during uranium acceleration. Upper panel indicates the numbers per day in 2017 and lower panel indicates those in 2018.

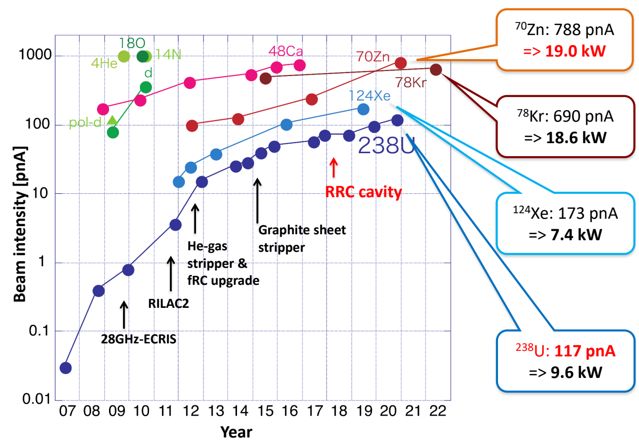

Figure 9: Evolution of the maximum beam intensity at the exit of the SRC up to summer 2022. The major R&D works for increasing the uranium beam are also indicated.

Figure 9 shows the evolution of the maximum beam intensity at the exit of the SRC from 2007 to summer 2022. After the upgrade of the RRC high-frequency systems, the uranium beam current achieved 117 pnA at the end of 2020, which corresponds to almost 10 kW. The beam power of other ions in the medium-mass regions now approaches 20 kW.

The modification of the RRC cavity resonator has improved the transmission efficiency of RRC to about 90%. This efficiency value of 90% excludes components that cannot be accelerated by the RRC in principle. This is because the upstream RILAC2 is operated at twice the frequency of the RRC, 36.5 MHz, and thus some of the beam components are injected in the deceleration phase of the RRC.

Recently, we have clearly seen a phenomenon in which the beam transmission efficiency decreases due to the influence of fluctuations in the receiving voltage. This occurs when the receiving voltage drops, but the cause is still unclear as it seems to have a compound cause. It has been found that the rf voltage of the RRC fluctuates very slightly despite the feedback. This may be due to an unstabilized filament current and anode voltage. At present, the rf voltage is fine-tuned manually by the operator when the receiving voltage fluctuates. We are planning to introduce a new digital low-level circuit in the RRC next year to further increase stability. Prior to this, a similar circuit was introduced into the injector RFQ, and it is clear that the new circuit has greatly improved stability. If this does not improve the situation, we will consider updating the filament power supplies.

ACKNOWLEDGEMENTS

The author is grateful to Dr. O. Kamigaito, Dr. N. Fukunishi, Dr. N. Sakamoto, Dr. K. Ozeki, and Dr. K. Suda for technical advice on this work. I would like to express my gratitude to the operators from SHI Accelerator Service Ltd. for their hard work preparing for the upgrade. I would like to thank Sumitomo Heavy Industries, Ltd. for their efforts in modifying the cavity.

REFERENCES

[1] Y. Yano, "The RIKEN RI Beam Factory Project: A status report", *Nucl. Instr. Meth. B*, vol. 261, pp. 1009–1013, 2007. doi:10.1016/j.nimb.2007.04.174

[2] H. Okuno *et al.*, "Progress of RIBF accelerators", *Prog. Theor. Exp. Phys.*, vol. 2012, p. 03C002, 2012. doi:10.1093/ptep/pts046

[3] Y. Yano, "Recent achievements at the RIKEN Ring Cyclotron", in *Proc. 13th Int. Conf. on Cyclotrons and their Applications (Cyclotrons'92)*, Vancouver, Canada, Jul. 1992, pp. 102–105.

[4] N. Inabe *et al.*, "Fixed-frequency ring cyclotron (fRC) in RIBF", in *Proc. 17th Int. Conf. on Cyclotrons and their Applications (Cyclotrons'04)*, Tokyo, Japan, Oct. 2004, pp. 200–202.

[5] T. Mitsumoto *et al.*, "Construction of the fRC sector magnet for RIKEN RI Beam Factory", in *Proc. 17th Int. Conf. on Cyclotrons and their Applications (Cyclotrons'04)*, Tokyo, Japan, Oct. 2004, pp. 384–386.

[6] N. Fukunishi *et al.*, "Acceleration of intense heavy ion beams in RIBF cascaded cyclotrons", in *Proc. 20th Int. Conf. on Cyclotrons and their Applications (Cyclotrons'13)*, Vancouver, Canada, Sep. 2013, pp. 1–6.

[7] J. Ohnishi *et al.*, "Construction status of the RIKEN intermediate-stage ring cyclotron (IRC)", in *Proc. 17th Int. Conf. on Cyclotrons and their Applications (Cyclotrons'04)*, Tokyo, Japan, Oct. 2004, pp. 197–199.

[8] H. Okuno *et al.*, "The superconducting ring cyclotron in RIKEN", *IEEE Trans. Appl. Supercond.*, vol. 17, pp. 1063–1068, 2007. doi:10.1109/TASC.2007.899864

[9] M. Odera *et al.*, "Variable frequency heavy-ion linac, RILAC", *Nucl. Instr. Meth. A*, vol. 227, pp. 187–195, 1984. doi:10.1016/0168-9002(84)90121-9

[10] O. Kamigaito *et al.*, "Construction of a booster linac for the RIKEN heavy-ion linac", *Rev. Sci. Instr.*, vol. 76, p. 013306, 2005. doi:10.1063/1.1834708

[11] K. Yamada *et al.*, "Beam commissioning and operation of new linac injector for RIKEN RI Beam Factory", in *Proc. 3rd Int. Particle Accelerator Conf. (IPAC'12)*, New Orleans, USA, May 2012, pp. 1071-1073.

[12] K. Suda *et al.*, "Design and construction of drift tube linac cavities for RIKEN RI Beam Factory", *Nucl. Instr. Meth. A*, vol. 722, pp. 55–64, 2013. doi:10.1016/j.nima.2013.04.007

[13] A. Goto *et al.*, "Injector AVF cyclotron at RIKEN", in *Proc. 12th Int. Conf. on Cyclotrons and their Applications (Cyclotrons1989)*, Berlin, Germany, May 1989, pp. 51–54.

[14] T. Kubo, "In-flight RI beam separator BigRIPS at RIKEN and elsewhere in Japan", *Nucl. Instr. Meth. B*, vol. 204, pp. 97–113, 2003. doi:10.1016/S0168-583X(02)01896-7

[15] T. Nakagawa *et al.*, "First results from the new RIKEN superconducting electron cyclotron resonance ion source (invited)", *Rev. Sci. Instr.*, vol. 81, p. 02A320, 2010. doi:10.1063/1.3259232

[16] Y. Higurashi *et al.*, "Recent development of RIKEN 28 GHz superconducting electron cyclotron resonance ion source", *Rev. Sci. Instr.*, vol. 85, pp. 02A953, 2014. doi:10.1063/1.4848976

[17] H. Imao, "Development of gas stripper at RIBF", in *Proc. 9th Int. Particle Accelerator Conf. (IPAC'18)*, Vancouver, Canada, Apr.-May 2018, pp. 41–46. doi:10.18429/JACoW-IPAC2018-MOZGBE1

[18] H. Hasebe *et al.*, "Development of a high-density highly oriented graphite stripper", *EPJ Web of Conf.*, vol. 229, p. 01004, 2020. doi:10.1051/epjconf/202022901004

[19] T. Fujisawa *et al.*, "The radiofrequency system of the RIKEN Ring Cyclotron", *Nucl. Instr. Meth. A*, vol. 292, pp. 1–11, 1990. doi:10.1016/0168-9002(90)91728-T

[20] O. Kamigaito *et al.*, "Recent progress in RIKEN RI Beam Factory", in *Proc. 22nd Int. Conf. on Cyclotrons and their Applications (Cyclotrons'19)*, Cape Town, South Africa, Sep. 2019, pp. 12–16. doi:10.18429/JACoW-Cyclotrons2019-MOB01

[21] H. Okuno *et al.*, "Operational experience and upgrade plans of the RIBF accelerator complex", in *Proc. 21st Int. Conf. on Cyclotrons and their Applications (Cyclotrons'16)*, Zurich, Switzerland, Sep. 2016, pp. 1–6. doi:10.18429/JACoW-Cyclotrons2016-MOA01

[22] R. Baartman, "Space charge limit in separated turn cyclotrons", in *Proc. 20th Int. Conf. on Cyclotrons and their Applications (Cyclotrons'13)*, Vancouver, Canada, Sep. 2013, pp. 305–309.

[23] CST Studio Suite, https://www.3ds.com/products-services/simulia/products/cst-studio-suite/

[24] W. Joho, "Application of the phase compression – phase expansion effect for isochronous storage rings", *Particle Accelerators*, vol. 6, pp. 41–52, 1974.